WILEY InterScience® DISCOVER SOMETHING GREAT

Quantum Chemical Simulation of Cytochrome P450 Catalyzed Aromatic Oxidation: Metabolism, Toxicity, and Biodegradation of Benzene Derivatives

P. N. D'YACHKOV,[1] N. V. KHARCHEVNIKOVA,[2] A. V. DMITRIEV,[3] A. V. KUZNETSOV,[1] V. V. POROIKOV[3]

[1]*Quantum Chemistry Laboratory, Kurnakov Institute of General and Inorganic Chemistry, Russian Academy of Sciences, Moscow, Russia*

[2]*Toxicology Laboratory, Institute of Human Ecology and Environmental Health, Russian Academy of Medical Sciences, Moscow, Russia*

[3]*Laboratory of Structure-Function Based Drug Design, Institute of Biomedical Chemistry, Russian Academy of Medical Sciences, Moscow, Russia*

Received 15 December 2006; accepted 4 April 2007
Published online 18 May 2007 in Wiley InterScience (www.interscience.wiley.com).
DOI 10.1002/qua.21416

ABSTRACT: The dependences of biological oxidation and toxicity of the mono- and multi-substituted benzene derivatives on the nature of substituents are studied using an oxenoid model and the quantum chemical calculations. According to this model, the P450 enzyme breaks the dioxygen molecules and generates the active atomic oxygen species (oxens); these species readily react with substrates. Using MO LCAO MNDO approach, we calculated the differences ΔE of the total energies of aromatic compounds and corresponding arene oxides containing tetrahedrally coordinated carbon atoms. We obtained that the ΔE values determine the positions of the enzyme mediated oxidation, rate of substrate biotransformation, and toxicity of the benzene derivatives. In addition to the "dynamic" reactivity index ΔE related to the enzyme-mediated substrate biotransformation, we calculated many standard "static" reactivity indices, corresponding to the substrate molecules in the starting equilibrium geometry (the energies of the occupied and unoccupied MOs, the effective atomic charges, the free valence indices, and the superdelocalizabilities). The arene oxide stability ΔE parameter is shown to be the most adequate characteristic of both the biological oxidation process and toxicity of benzenes. The ΔE parameters were also used successfully to describe the features of di- and tri-chlorinated biphenyls bacterial metabolism. Int J Quantum Chem 107: 2454–2478, 2007

Key words: MO LCAO MNDO approach; benzene derivatives; chlorinated biphenyls; metabolism; biological oxidation; P450 monooxygenase system; toxicity

Correspondence to: P. N. D'yachkov; e-mail: p_dyachkov@rambler.ru

Introduction

Many chemical compounds require a bioactivation to exert the toxic effects and initiate the tumors [1–10]. Particularly, a concept of enzymatic activation of the procarcinogens to the proximate and ultimate carcinogens has been approved by the in vitro and in vivo studies, as well as by structure-carcinogenic activity relationships obtained using quantum chemical parameters in the series of polycyclic aromatic compounds and their derivatives [11–26], haloidalkanes and haloidalkenes [27–32]. The oxidation catalyzed by a microsomal P450 monooxygenase system is a common mechanism of the xenobiotics activation. The P450 enzymes take part in the detoxication, biodegradation, and bioactivation reactions of chemicals. An iron(III) porphyrin complex forms an active site of the cytochrome P450 [33–35]. The problems of the cytochrome P450 structure-function relationships were treated in many books and papers on enzymology, xenobiochemistry, and toxicology [32–41]. Not so much is known about an influence of substrate electronic structure on its enzymatic oxidation.

The benzene derivatives are known to be the typical substrates of the cytochrome P450 mediated hydroxylation. Figure 1 shows the important features of the multistage mechanism of hydroxylation of these molecules [2, 3]. Experiments show that a rate of oxidation, a yield of the hydroxylated products, and the toxicity of benzene derivatives C_6H_5X depend strongly on a nature of substituent X. In this article, we study these dependences on the basis of quantum chemical calculations using the so-called oxenoid model [42]. According to this model, the P450 enzyme breaks the dioxygen molecule and generates the active atomic oxygen species (oxens) [43]. The oxens readily react with substrates. For the molecules with conjugated and isolated π-bonds, some features of oxenoid model were studied from the experimental and quantum chemical point of view [44–46]. On the basis of these data, we suggest that the stability of the intermediate IV containing one tetrahedrally coordinated carbon atom relative to the original molecule I is the factor that determines the rate of enzyme mediated substrate biotransformation. Using the MO LCAO MNDO approach, we have calculated the total energies of molecules I and arene oxides IV (E_I and E_{IV}, respectively). A difference $\Delta E = E_{IV} - E_I$ approximately determines an activation energy of the oxidation reaction [42]. In our calculations of the benzene derivatives I, we have optimized only the substituent geometries. The structure of distorted benzene ring of the intermediates IV was taken from the paper [42]. The geometry of substituent in the intermediate IV is suggested to be the same as the geometry of this substituent in the initial molecule of substituted benzene I.

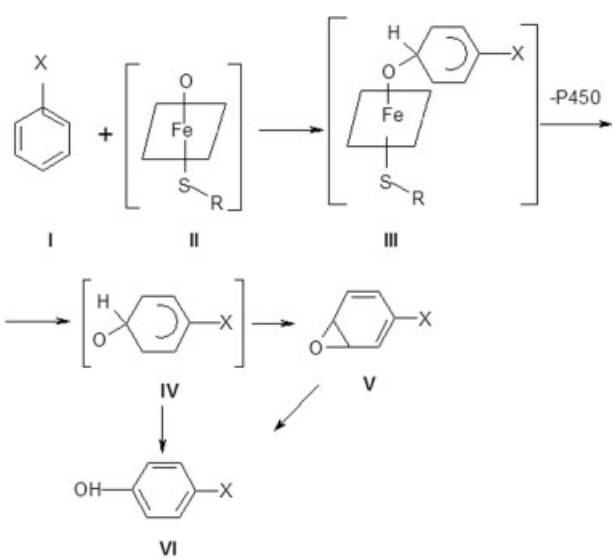

FIGURE 1. Mechanism of aromatic hydroxylation by cytochrome P450.

Positions of Hydroxylation

Table I shows the calculated values of activation energies ΔE for the addition of oxygen to the C atoms of monosubstituted benzenes together with the experimental in vivo and in vitro data on the hydroxylation of benzene derivatives C_6H_5X. The ΔE value of benzene C_6H_6 is taken as the energy reference point ($\Delta E(C_6H_6) = 0$). The negative ΔE values point on the stabilization of the arene oxide derivative of the C_6H_5X molecule relative to that of the benzene. The positive ΔE value points on arene oxide destabilization. Let us consider how the calculated ΔE values correlate with the experimental hydroxylation data. As follows from the developed model, the enzyme activated oxygen species should be bonded preferentially to those C atoms, for which the ΔE values are minimal and, consequently, the inter-

TABLE I

Formation energies (ΔE) for arene oxides and rate of biological oxidation of benzene derivatives C_6H_5X.

No	Substituent X	ΔE (eV) and amount of phenols formed (% of the dose administrated) *ortho*	*meta*	*para*	Object of experimentation	Reference
1	$N(C_2H_5)_2$	ΔE −0.79	0.12	−0.76		
		a found	—	found	rat, dog	53
2	NH_2	ΔE −0.78	0.1	−0.6		
		7–10	0.1	40–55	rabbit	32, 53
		4	—	46	guinea pig	32
		19	—	48	rat	32
		6	—	56	hamster	32
		26	—	28	polar cat	32
		18–25	—	9–11	dog	32
		32	—	14	cat	53, 54
		—	—	20	in vitro	47
		e 0.9–8.3	—	1.9–22.2	perfused liver	55
3	OH	ΔE −0.68	0.18	−0.37		
		0.5–1.0	—	10	rat	32, 53
		a found	—	found	rabbit	56
4	$N(CH_3)(C_2H_5)$	ΔE −0.54	0.1	−0.63		
		—	—	2.5–3.9	in vitro	57
5	OC_2H_5	ΔE −0.37	0.13	−0.48		
		a —	—	found	dog	53
6	OCH_3	ΔE −0.25	0.14	−0.39		
		less	—	more	rat	53
		1	—	10	in vitro	47
		19.5	2	68.5	in vitro	47
		less	—	more	in vitro	55
7	NHCHO	ΔE −0.18	0.16	−0.34		
		traces	—	3.2	in vitro	47
8	$NHCONH_2$	ΔE 0.11	0.13	−0.33		
		—	—	21.6	in vitro	47
9	$NHCOCH_3$	ΔE 0	0.13	−0.32		
		traces	—	70	rabbit	53
		a —	—	found	human	53
		a more	—	less	dog	53
		traces	—	27.2	in vitro	47
10	$CH{=}CH_2$	ΔE −0.17	0	−0.14		
		a —	—	found	not listed	58, 65
		—	—	0.1	rabbit	59
11	F	ΔE −0.14	0.19	−0.12		
		a traces	—	found	rat	53
		0.08	0.05	0.03	in vitro	47
12	C_6H_5	ΔE −0.07	0	−0.17		
		0.4	—	10	in vitro	47
13	$CH_3CH{=}CH_2$	ΔE −0.04	−0.02	−0.1		
		b —	—	20	dog	53
14	C_2H_5	ΔE −0.03	−0.01	−0.08		
		—	—	0.3	rat	59

(*continued*)

TABLE I
(Continued)

No	Substituent X	ΔE (eV) and amount of phenols formed (% of the dose administrated) *ortho*	*meta*	*para*	Object of experimentation	Reference
15	CH_3	ΔE −0.03	0.14	−0.39		
		c 3.54	1.27	32.6	human	58, 60
		c 1.34	0.37	6.4	human	61
		c 0.38	0.05	6.43	human	62
		0.04–0.11	—	0.4–1.0	rat	59
		0.3	—	0.3	in vitro	47
		d 17	1.5	19	in vitro	63
		a —	—	found	rats	64
		a —	—	found	human	69
16	$NHCOCF_3$	ΔE 0.02	0.2	−0.15		
		—	—	3.2	in vitro	47
17	$CH_2CH(NH_2)_2$	ΔE 0.38	0	−0.06		
		—	—	3	human	32
		—	—	60	rat	32
18	$CONH_2$	ΔE 0.02	0	0.15		
		d 1	10	2	guinea pig	47
19	Cl	ΔE 0.14	0.1	0.1		
		1.6	3.6	4.8	rat	70
			1.6	3,4-diol		66, 67
		0.1	—	2–3	rat	32, 53
20	COOH	ΔE 0.35	0.04	0.22		
		a —	traces	—	in vitro	47
21	CN	ΔE 0.27	0.1	0.16		
		a traces		traces	in vitro	47
22	NO_2	ΔE 0.48	0.19	0.38		
		0.1	7.8–9	8–9	rabbit	32
		—	8.4–10.2	13–19.9	rat	68
		—	6.7	7.2	mouse	68
		a —	—	found	guinea pig	47
		a —	—	traces	in vitro	47
		d 2–16	33–34	49–54	in vitro	63

a - There is no quantitative estimate of phenols concentration in the experimental article.
b - Concentration of *para*-hydroxyphenylacetic acid.
c - Concentration of phenols in urine expressed in mg/l.
d - Ratio of isomer concentration.
e - Numerical data in nmol/min/g liver.

mediates IV are more stable. All the compounds presented in Table I can be divided into four groups according to the values of the $\Delta E(ortho)$, $\Delta E(meta)$, and $\Delta E(para)$:

i. Molecules C_6H_5X with X = NH_2, OH, $N(CH_3)(C_2H_5)$, OC_2H_5, OCH_3, NHCHO, $NHCONH_2$, $NHCOCH_3$, $CHCH_2$, and F. In this case, the $\Delta E(meta) > 0$; thus, the *meta*-position is deactivated and the *meta*-phenols are not expected to be formed. In agreement with theory, the *meta*-phenols are either not observed or present in minor quantity in experiment. The *ortho*- and *para*-positions are activated, because $\Delta E(ortho) < 0$ and $\Delta E(para) < 0$; therefore, the *ortho*- and *para*-phenols are

readily formed during the metabolism of these compounds. The concentration of *para*-phenols is larger than that of *ortho*-phenols, possibly, due to the steric interactions of active oxygen and substituent X in the *ortho*-position;

ii. Compounds with X = alkyl and X = CH_3—CH═CH. Here, $\Delta E(para) < 0$, $\Delta E(meta) < 0$, $\Delta E(ortho) < 0$, and $\Delta E(para) < \Delta E(ortho) < \Delta E(meta)$; i.e., every position is activated, but the para-position is the most active one. The experimental data are in excellent agreement with all these predictions;

iii. For compound with X = $CH_2CHNH_2CH_3$, the *para*-position is the only activated one, and biotransformation of this molecule leads to the formation of *para*-phenol;

iv. Compounds with X = $CONH_2$, COOH, Cl, and CN. Here, the $\Delta E(ortho) > 0$, $\Delta E(para) > 0$, $\Delta E(meta) > 0$, and every position is deactivated. However, the *meta*-positions are the most active ones, and the *meta*-phenols are expected to be formed easier (*meta*- and *para*-phenols for the C_6H_5Cl). The predicted relative concentrations of isomers correlate with experimental data for $C_6H_5CONH_2$, C_6H_5Cl, and C_6H_5COOH. Correlation is not so good for compounds with the strongest destabilizing substituents X = NO_2 and CN.

Rate of Phenol Formation Versus Arene Oxide Stability

Let us turn to the quantitative relationships between the stability parameter ΔE of the arene oxide intermediates IV and the concentrations C of the phenols formed in the standard in vitro test using the microsomes of rat and hamster [47]. Figure 2 shows that there is the linear correlation between the lg$C$ (mg/l) and ΔE (eV). The growth of the ΔE from −0.6 to +0.2 eV points on the destabilization of the intermediate IV and is linked to the decrease of the metabolite concentrations. The regression equation has the following form

$$\lg C = -4.869\,\Delta E - 1.075,\ r = 0.89,\quad n = 15,\ P < 0.001. \quad (1)$$

It should be pointed that only a trace of the hydroxylated products is observed in the microsomal test for the compounds C_6H_5COOH, $C_6H_5NO_2$, and C_6H_5CN having the largest ΔE values [19].

(Here and below, an application of molar concentrations for the C and LC_{50} and molar doses for LD_{50} virtually does not change the correlation coefficients in the equation for biological effects, as there are only small variations of logarithm of the molecular masses in the series of benzene derivatives under consideration).

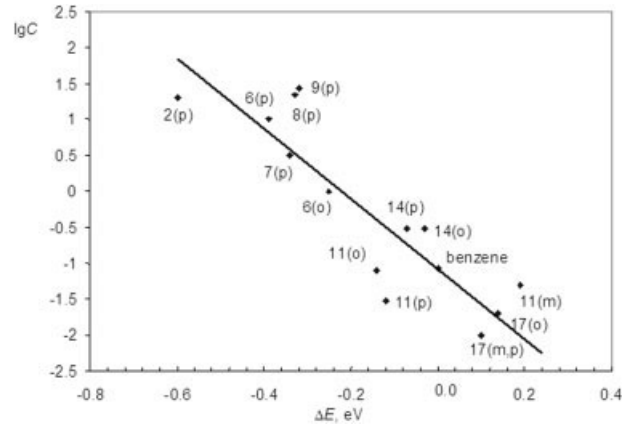

FIGURE 2. Dependence of the concentration C (mg/l) of phenols formed on the stability of arene oxide intermediates IV. Here, the numbers correspond to compounds in Table I.

Toxicity Versus Arene Oxides Stability

In this section, we focus on analysis of the acute toxicity of benzene derivatives from the point of view of stability of the intermediates IV. The experimental mean lethal doses (LD_{50}) for oral administration and the mean lethal concentrations (LC_{50}) for inhalatory administration of benzene derivatives are presented in Table II together with the calculated values of the minimal energy $\Delta E_{min} = \min\{\Delta E(ortho), \Delta E(meta), \Delta E(para)\}$ of the arene oxide formation. Figure 3 shows that the increase of ΔE_{min} results in the increase of the experimental values of the LC_{50} and LD_{50}. The linear regression equations are

$$\lg LD_{50} = 1.18\,\Delta E_{min} + 3.61;\quad r = 0.78,\ n = 23,\ P < 0.001, \quad (2)$$

$$\lg LC_{50} = 3.08\,\Delta E_{min} + 4.62;\quad r = 0.93,\ n = 12,\ P < 0.001 \quad (3)$$

TABLE II

Formation energy of the tetrahedral intermediate and toxicity of benzene derivatives C_6H_5X.

Compound	Substituent X	ΔE_{min}	$lgLD_{50}$ Mice (mg/kg)	$lgLD_{50}$ Rats (mg/kg)	$lgLC_{50}$ Mice (mg/m^3)	$lgLC_{50}$ Rats (mg/m^3)
N-Ethylaniline	NHC_2H_5	–0.80	2.7	2.46	—	—
Aniline	NH_2	–0.78	2.66	2.64	—	—
Phenol	OH	–0.68	2.63	2.71	2.25	2.52
Isopropylbenzene hydroperoxide	$C(CH3)_2OOH$	–0.64	2.53	—	—	—
Phenetole	OCH_2CH_3	–0.48	3.34	—	—	—
Anisole	OCH_3	–0.39	3.46	3.62	3.49	3.95
Phenoxyacetic acid	$OCOCH_3$	–0.38	3.57	3.57	—	—
N-methyl-*N*-phenyl urea	$NHCONHCH_3$	–0.37	—	3.4	3.64	—
Dimethylphenyl carbinol	$C(CH_3)_2OH$	–0.36	3.29	3.32	—	—
N-phenyl-*N*,*N*-dimethylurea	$NHCON(CH_3)_2$	–0.34	—	3.88	—	—
Acetanilide	$NHCOCH_3$	–0.32	—	3.23	—	—
Tetrafluorethyl ether of phenol	OC_2F_4H	–0.22	3.56	3.70	4.28	4.39
Biphenyl	C_6H_5	–0.17	—	3.65	—	—
Styrene	$CH{=}CH_2$	–0.17	3.70	—	3.98	4.07
α-Methylstyrene	$C(CH_3){=}CH_2$	–0.16	3.69	—	—	—
Fluorobenzene	F	–0.14	3.64	—	4.44	—
Isopropylbenzene	i-C_3H_7	–0.11	3.15	—	4.40	—
Propylbenzene	C_3H_7	–0.08	3.72	3.88	—	—
Ethylbenzene	C_2H_5	–0.08	3.54	—	4.54	4.76
Toluene	CH_3	–0.07	3.60	.81	4.51	4.60
Acetophenone	$COCH_3$	–0.07	3.13	3.42	—	—
Isobutylbenzene	i-C_4H_9	–0.06	3.56	3.58	4.42	—
Benzyl alcohol	CH_2OH	–0.03	3.56	3.58	4.42	—
Benzene	H	0.00	3.66	3.81	4.65	4.81
Benzoic acid	COOH	0.04	3.21	3.52	—	—
Benzaldehyde	CHO	0.02	3.31	3.38	—	—
Chlorobenzene	Cl	0.10	3.36	3.52	4.28	—
Benzonitrile	CN	0.10	—	2.9	—	—
Benzotrichloride	CCl_3	0.11	3.11	—	1.78	2.18
Benzotrifluoride	CF_3	0.12	4.0	4.18	5.0	4.85
Benzoyl chloride	CClO	0.13	—	—	—	3.27
Nitrobenzene	NO_2	0.20	—	2.81	—	—

Values of the LD_{50} and LC_{50} are taken from [48].

for mice and

$$lgLD_{50} = 1.24\ \Delta E_{min} + 3.70; \quad r = 0.77, n = 22, P < 0.001, \quad (4)$$

$$lgLC_{50} = 2.99\ \Delta E_{min} + 4.79; \quad r = 0.95, n = 8, P < 0.001 \quad (5)$$

for rats.

Arene Oxide Stability Versus Static Indices for Toxicology Prediction

In addition to the "dynamic" reactivity index ΔE related to the enzyme-mediated substrate biotransformation, we have calculated the following standard "static" reactivity indices: the energies of the highest occupied (E_{HOMO}) and lowest unoccupied molecular orbitals (E_{LUMO}), the energy gap E_g

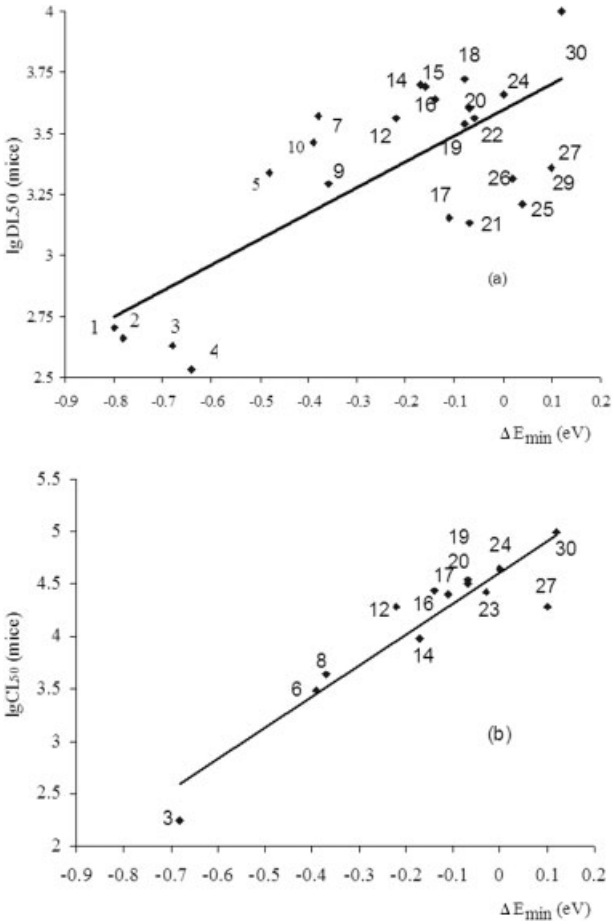

FIGURE 3. Dependencies of the mean oral lethal doses LD_{50} (mg/kg) (a) and mean inhalatory lethal concentrations LC_{50} (mg/m^3) (b) for mice on the parameter ΔE_{min} in the series of benzene derivatives. Numbers correspond to compounds identified in Table II.

between the HOMO and LUMO, the maximum value of effective charge of the five benzene ring C atoms not bonded to substituent X (Q_{max}), the sum of absolute values of effective charges of the C atoms ($\Sigma_i|Q_i|$), the free valence index (F) of the benzene ring C atoms, the maximum electrophilic (S^E_{max}) and nucleophilic (S^N_{max}) superdelocalizabilities of the C atoms, and the sums of electrophilic ($\Sigma_i S^E_i$) and nucleophilic ($\Sigma_i S^N_i$) superdelocalizabilities of the benzene ring C atoms. All these parameters refer to the properties of the molecule in the starting equilibrium geometry, but not to a transformation of substance in the chemical or biochemical reactions.

Table III shows some of these parameters. In this Table, the values of hydrophobicity constants [48] often used to describe the toxicants distribution between the hydrophobic and hydrophilic phases of biological system are presented too. The results of calculations of the monosubstituted benzene derivatives show that there are no correlations between the toxicity or biooxidation characteristics and the following static indices: Q_{meta}, E_{HOMO}, E_{LUMO}, E_g, $\Sigma_i S^N_i$, $\Sigma_i S^E_i$, F_{meta}, and S^E_{max}. The correlations of the biological effects with the parameters Q_{max}, $\Sigma_i|Q_i|$, Q_{ortho}, Q_{para}, $F_{max} = \max\{F_{ortho}, F_{para}\}$, and S^N_{max} are somewhat better; however, the values of correlation coefficients are lower than those of the ΔE (Table IV). In the series of static parameters, the highest values of the correlation coefficients are obtained for the F_{max} and S^N_{max} indices. At first glance, it would seem that there is reasonable correlation of the toxicity and the free valence index F. However, according to values of F_{max}, the carbon atom located in the *ortho*-position to substituent X must be the most reactive one for all the investigated compounds. Judging by the values of F_{max}, all the monosubstituted benzene derivatives have to form the *ortho*-phenols, but this is not true. For the same reason, the S^N_{max} parameter pointing on the most active C atom in the reactions of the benzene derivatives with the nucleophilic particles is inadequate. The positions of hydroxylation predicted on the basis of the S^N_{max} values do not correlate with experimental data presented in Table I. Using the value of Q_{max}, one cannot adequately describe the preferred hydroxylation position of the monosubstituted benzenes too. According to the values of Q_{max}, all the substances fall into two groups: (*i*) those to be hydroxylated in the *ortho*-position (compounds 1−8, 10−12, and 16 in Table III) and (*ii*) those to be hydroxylated in the *meta*-position (other compounds in this Table); this result is in conflict with the data on the biological oxidation of benzene derivatives (Table I). The correlation coefficients for the parameters LC_{50} and LD_{50} versus ΔE are greater than those for the toxicity versus hydrophobicity π (Table IV). In conclusion, the arene oxide stability determines the biological oxidation and toxicity of monosubstituted benzenes; the ΔE parameter seems to be the most adequate characteristic of the hydroxylation process.

Toxicity of Multiple Substituted Benzene Derivatives

To test further the validity of the model developed, we have calculated the values of ΔE for the 31 multiply substituted benzene derivatives C_6H_4XY, where X and Y are Cl, NH_2, NO_2, alkyl, and OCH_3. Using the Eqs. (2) and (3), we have calculated the

TABLE III

The values of π_R, ΔE_{min}, and quantum chemical static reactivity indices for the mono substituted benzene derivatives C_6H_5X.

Compound	Substituent X	π_R	Q_{para}	Q_{ortho}	Q_{max}	$\Sigma\|Q\|$	F_{max}	F_{para}	S^N_{max}	ΔE_{min}
N-Ethylaniline	NHC_2H_5	0.08	0.116	0.142	0.142 o	0.423	0.439	0.4089	0.0565 o	–0.80 o
Aniline	NH_2	–1.23	0.114	0.135	0.135 o	0.412	0.4374	0.4084	0.0562 o	–0.78 o
Phenol	OH	–0.67	0.097	0.145	0.145 o	0.373	0.4348	0.4044	0.0537 o	–0.68 o
Isopropylbenzene hydroperoxide	$C(CH3)_2OOH$	—	–0.55	0.073	0.073 o	0.262	0.4017	0.3996	0.0502 o	–0.64 o
Phenetole	OCH_2CH_3	0.38	0.098	0.145	0.145 o	0.377	0.4298	0.4045	0.0538 o	–0.48 p
Anisole	OCH_3	–0.02	0.09	0.133	0.133 o	0.353	0.4253	0.4033	0.0526 o	–0.39 p
Phenoxyacetic acid	$OCOCH_3$	—	0.092	0.146	0.146 o	0.36	0.4283	0.4036	0.0527 o	–0.38 p
N-methyl-*N*-phenylurea	$NHCONHCH_3$	—	0.084	0.103	0.103 o	0.361	0.4210	0.4037	0.0531 o	–0.37 p
Dimethylphenyl carbinol	$C(CH_3)_2OH$	—	0.053	0.023	0.061 m	0.252	0.4186	0.4059	0.0487 o	–0.36 o
N-phenyl-*N*,*N*-dimethylurea	$NHCON(CH_3)_2$	—	0.085	0.103	0.103 o	0.361	0.4211	0.4037	0.0531 o	–0.34 p
Acetanilide	$NHCOCH_3$	–0.97	0.083	0.100	0.100 o	0.357	0.4205	0.4037	0.0526 o	–0.32 p
Tetrafluorethyl ether of phenol	OC_2F_4H	—	0.07	0.116	0.116 o	0.294	0.4182	0.4023	0.0514 o	–0.22 p
Biphenyl	C_6H_5	1.96	0.055	0.043	0.061 m	0.264	0.4122	0.4033	0.0487o,m	–0.17 p
Styrene	$CH{=}CH_2$	0.82	0.054	0.040	0.064 m	0.262	0.4160	0.4041	0.0521 o	–0.17 o
α-Methylstyrene	$C(CH_3){=}CH_2$	—	0.054	0.043	0.062 m	0.263	0.4152	0.4038	0.0487o,m	–0.16 p
Fluorobenzene	F	0.14	0.071	0.089	0.089 o	0.32	0.4154	0.4022	0.0477 p	–0.14 o
Isopropylbenzene	*i*-C_3H_7	1.53	0.057	0.045	0.062 m	0.265	0.4038	0.4005	0.0488 m	–0.11 p
Ethylbenzene	C_2H_5	1.02	0.056	0.043	0.062 m	0.262	0.4042	0.4007	0.0486 m,p	–0.08 p
Toluene	CH_3	0.56	0.055	0.041	0.062 m	0.262	0.4045	0.4008	0.0488 m	–0.07 p
Acetophenone	$COCH_3$	–0.55	0.026	0.012	0.079 m	0.207	0.4156	0.4046	0.048 m	–0.07 m
Isobutylbenzene	i-C_4H_9	—	0.057	0.042	0.062 m	0.265	0.4037	0.4004	0.0488 m	–0.06 p
Benzyl alcohol	CH_2OH	–1.03	0.050	0.040	0.072 m	0.244	0.4046	0.4008	0.0495 m	–0.03 p
Benzene	H	0	0.059	0.059	0.059	0.297	0.3987	0.3987	0.0487	0
Benzoic acid	COOH	–0.32	0.021	0.090	0.082 m	0.201	0.4143	0.4051	0.0478 m	0.04 m
Benzaldehyde	CHO	–0.65	0.021	0.014	0.081 m	0.196	0.4183	0.4057	0.0497 o	0.02 m
Chlorobenzene	Cl	0.71	0.050	0.040	0.056 m	0.243	0.4055	0.4020	0.0469 m	0.10 m,p
Benzonitrile	CN	–0.57	0.032	0.017	0.070 m	0.201	0.4116	0.4042	0.0467 m	0.10 m
Benzotrichloride	CCl_3	—	0.022	0.050	0.070 m	0.168	0.4097	0.4054	0.0467 m	0.11 m
Benzotrifluoride	CF_3	0.88	0.023	0.050	0.070 m	0.212	0.4048	0.4035	0.0464 m	0.12 m
Benzoyl chloride	CClO	—	0.011	0.015	0.080 m	0.200	0.4182	0.4080	0.0465 m	0.13 m
Nitrobenzene	NO_2	–0.28	0.010	0.014	0.074 m	0.187	0.4177	0.4093	0.0467 m	0.20 m

For Q_{max}, S^N_{max} and ΔE_{min}, the positions of C atom in benzene ring with maximal value of Q_{max}, S^N_{max} and minimal value of ΔE are indicated.

LD_{50} and LC_{50} values for mice. A comparison of the theoretical and experimental characteristics shows that the ΔE values adequately predict the toxicity of the multiple substituted compounds (Table V). There are only minor disagreements: (*i*) in the case of resorcine, the experimental value of LD_{50} is six times larger than the theoretical one; (*ii*) for the *ortho*-chlorobenzene, the theoretical value of LD_{50} is about 10 times overestimated; (*iii*) the data on the *para*-chlorophenol are ambiguous: for rats, there is complete agreement between the theoretical and experimental values of LC_{50}, but analogous experimental value for mice is 10 times lower.

Bio-Oxidation of Phenols

In biological systems, phenols can be further hydroxylated yielding the corresponding diols. Table VI shows in vivo data on the positions of hydroxylation of 16 substituted XC_6H_4OH phenols together with the theoretical ΔE values. The hydroxylation takes place

TABLE IV

Linear correlation coefficients between biological activity parameters (LD_{50} and LC_{50} for mice and rats) and reactivity and lipophilicity indices for benzenes derivatives C_6H_5X.

Parameter of toxicity	Correlation coefficient *r* and number of observations *n*	ΔE_{min}	π_R	Q_{max}	$\Sigma\|Q\|$	Q_{ortho}	Q_{para}	$F_{max} = F_{ortho}$	F_{para}	S^N_{max}
$\lg LD_{50}$ (mg/kg) mice	*r*	0.78*	0.6	–0.44	–0.43	–0.44	−0.47	−0.38	−0.39	−0.56
	n	23	16	23	23	23	23	23	23	23
$\lg LD_{50}$ (mg/kg) rats	*r*	0.77*	0.57	−0.58	−0.54	−0.53	−0.57	−0.70*	−0.70*	−0.67*
	n	23	17	22	22	22	22	22	22	22
$\lg LC_{50}$ (mg/m^3) mice	*r*	0.93*	0.69	−0.82*	−0.82*	−0.81*	−0.84*	−0.86*	−0.52	−0.78
	n	12	10	12	12	12	12	12	12	12
$\lg LC_{50}$ (mg/m^3) rats	*r*	0.95*	0.75	−0.80	−0.74	−0.77	−0.91*	−0.79	−0.64	−0.84
	n	8	7	12	12	12	12	12	12	12

* $P < 0.001$.

at positions corresponding to the minimal ΔE values. This process is inhibited for the C atoms located at the *meta*-positions relative to the OH-groups ($\Delta E > 0$), and this type of oxidation is not observed experimentally. The OH-group activates both *ortho*- and *para*-positions ($\Delta E_{ortho} < \Delta E_{para} < 0$), and the *ortho*- and *para*-dihydroxilated products are formed.

Aromatic Hydroxylation of Compounds From Metabolite Database

A Metabolite v.2001.1 database (MDL Information Systems Inc.) contains information on the in vivo and in vitro biotransformation of many thousands drugs and industrial chemicals. More than two thousands transformations are referred in the database to "Aromatic Hydroxylation". We use this information to further test the ability of our approach to recognize experimentally observed transformations. We randomly selected 24 compounds, which can be regarded as substituted benzenes. All these compounds contain both observed and unobserved sites of benzene ring hydroxylation.

We ranked all potential transformations by the ΔE value. Ideally, real (experimentally observed) transformation should have lower rank than unreal transformation. The accuracy of prediction was estimated as

$$\mathrm{IAP} = \frac{N(\mathrm{rank_r} < \mathrm{rank_u})}{N_r \cdot N_u} \cdot 100\%.$$

Here, $N(\mathrm{rank_r} < \mathrm{rank_u})$ is the number of cases when a real transformation has lower rank then an unreal transformation; the N_r and N_u are the numbers of real and unreal transformations of the substrate, respectively. This statistics was calculated for every particular substrate and averaged by number of substrates in the validation set. The averaged value accounts for 91.2%.

Thus, the statistical analysis shows that the predicted hydroxylation positions agree with those observed in experiments in the majority of cases. In some cases, there are no experimental data for hydroxylation of the positions predicted to be active.

Let us discuss in greater detail the results presented in Table VII. For the compound 1, the oxenoid model shows that the oxidation reaction should take place in the *para*-position relative to the substituent. This process one observes in vitro and in human. In the compound 2, there are two possible oxidation positions of the benzene ring hydroxylation; however, the calculations show that hydroxylation in the *meta*-position is energetically more favorable, and precisely the *meta*-phenol is detected in experiment.

In the case of compound 3, the para-hydroxylation is more energetic than that in the *ortho*- and

TABLE V

Experimental and calculated in terms of Eqs. (1) and (2) toxicity parameters for multiple substituted benzene derivatives.

No	Substance	ΔE_{min}	$lgLD_{50}$, mg/kg		$lgLC_{50}$, mg/m^3	
			exp.	theor.	exp.	theor.
1.	*m*-Chloroaniline	−0.69	2.57	2.8	—	2.49
2.	*p*-Chloroaniline	−0.83	2.6	2.63	—	2.06
3.	*m*-Nitrochlorobenzene	−0.69	—	2.8	—	2.49
4.	*p*-Nitrochlorobenzene	−0.83	2.64	2.63	—	2.06
5.	*m*-Aminobenzotrifluoride	−0.52	2.34	3.0	2.84	3.02
6.	*m*-Nitrobenzotrifluoride	−0.52	2.72	3.0	2.94	3.02
7.	*m*-Methylaniline	−0.82	2.87	2.64	—	2.09
8.	*p*-Methylaniline	−0.81	2.43	2.65	—	2.13
9.	*m*-Nitrotoluene	−0.82	2.9	2.64	2.63	2.09
10.	*p*-Nitrotoluene	−0.81	3.11	2.65	2.62	2.13
11.	*o*-Aminophenol	−0.81	2.62	2.65	—	2.13
12.	*p*-Aminophenol	−0.73	3.18	2.75	—	2.37
13.	*p*-Nitroaniline	−0.68	—	2.81	—	2.53
14.	*o*-Nitrophenol	−0.81	3.32	2.65	—	2.13
15.	*p*-Nitrophenol	−0.73	2.58	2.75	—	2.37
16.	*p*-Chlorobenzotrifluoride	+0.14	4.06	3.78	4.30	5.05
17.	*p*-Chlorotoluene	+0.03	3.60	3.65	4.79	4.71
18.	*o*, *m*, *p*-Xilene (on ortho)	−0.18	3.63	3.4	—	4.07
19.	*o*-ethyltoluene	−0.12	—	3.47	4.73	4.25
20.	*p*-Chlorophenol	−0.64	—	2.85	1.04	2.65
21.	*o*-Methylphenol	−0.72	2.54	2.78	2.25	2.46
22.	*m*-Methylphenol	−0.70	2.54	2.73	—	2.31
23.	*p*-Methylphenol	−0.58	2.54	2.78	—	2.46
24.	Pyrocatechol	−0.56	2.15	2.95	—	2.90
25.	Resorcin	−0.80	2.38	2.67	—	2.16
26.	Hydroquinone	−0.47	2.56	3.04	—	3.14
27.	*m*-Methoxyphenol	−0.69	2.49	2.80	—	2.49
28.	*o*-Dichlorobenzene	0.07	2.70	3.69	—	4.84
29.	*p*-Hydroxybenzaldehyde	−0.61	3.43	2.90	—	2.74
30.	*o*-Propylphenol	−0.66	2.55	2.83	—	2.59
31.	*p*- Propylphenol	−0.58	2.54	2.93	—	2.83
32.	2,6-Dimethylphenol	−0.45	2.65	3.08	—	3.23
33.	3,5-Dimethylphenol	−0.59	2.92	2.91	—	2.80

Values of the LD_{50} and LC_{50} are taken from [48].

meta-positions, and the *para*-phenol was observed in variety of in vivo and in vitro experiments.

According to these calculations and in agreement with the experiment, hydroxylation of the compound 4 should take place in the *ortho*- and *para*-positions. Here, the ΔE_{ortho} and ΔE_{para} parameters are negative; thus, these positions are activated in relation to benzene. The table shows that the *ortho*- and *para*-phenols are found in this case. A rate of hydroxylation reaction is very high; in rabbits, up to 70% of the dose administrated is oxidized forming the *ortho*- and *para*-phenols.

In the aniline $C_6H_5NH_2$, there is a strong activating substituent NH_2. All free positions are activated and all three metabolite isomers of the $C_6H_5NH_2$ are observed in the biological experiments. The ΔE_{ortho} and ΔE_{para} values are the smallest ones in the series of considered compounds. That is the reason why the experimental rate of metabolism of this compound is very high.

For the compound 6 containing two benzene rings, the most stable intermediates correspond to the oxygen atom located in the *para*-position with respect to the substituents in both rings. In

TABLE VI

Energies of arene oxide formation (Δ*E*, eV) for different C atoms and experimentally observed products of hydroxylation of the substituted phenols.

No	Phenols and values of Δ*E*	Product of hydroxylation	Condition of experiment	Reference
1	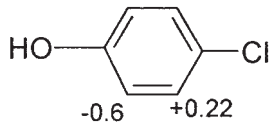 *para*-chlorophenol	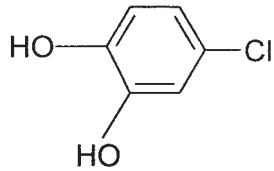 4-chlorocatechol	rabbit	53
2	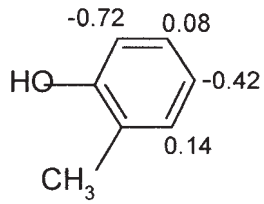 *ortho*-cresol	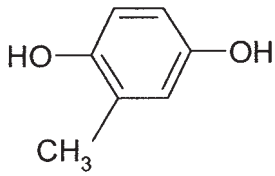 2,5-dihydroxytoluene	rabbit	53
3	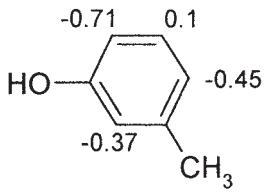 *meta*-cresol	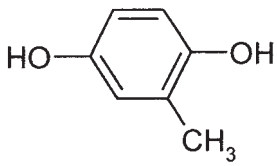 2,5-dihydroxytoluene	rabbit	53
4	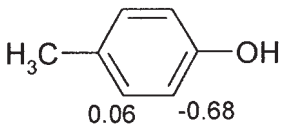 *para*-cresol	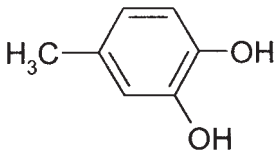 3,4-dihydroxytoluene	rabbit	53, 32
5	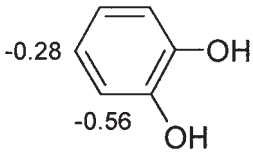 pyrocatechol	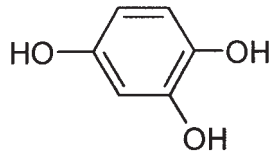 oxyhydroquinone	rabbit	32

(*continued*)

vivo and in vitro experiments substantiate this conclusion.

For the compound 7, the intermediate corresponding to the *ortho*-hydroxylation is the most stable, and the appropriate metabolite is found using the microsomes. However, the products of *para*- and *meta*-hydroxylation are detected in this case too, because the Δ*E* values are small for all aromatic position and only slightly differ from that of benzene.

The only metabolite with OH-group in the *ortho*-position to the OH-group of substrate is detected experimentally for the compound 8. According to the calculations, this position is activated with respect to benzene.

In the case of compound 9, the energies of the *para*- and *ortho*-intermediates differ by 1 kcal/mol; however, only *para*-phenol is seen in vitro. The absence of the ortho-isomer can be attributed to

TABLE VI
(Continued)

No	Phenols and values of ΔE	Product of hydroxylation	Condition of experiment	Reference
6	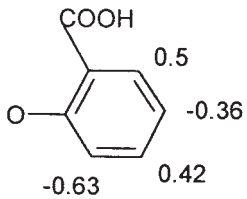 Salicylic acid	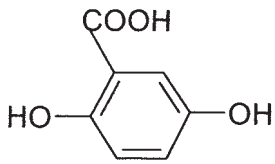 2,5-dihydroxybenzoic acid		53, 32
		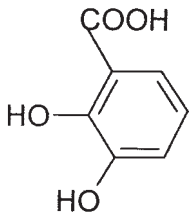 2,3-dihydroxybenzoic acid	human	
		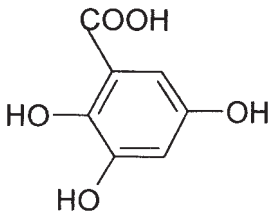 2,3,5-trihydroxybenzoic acid		
		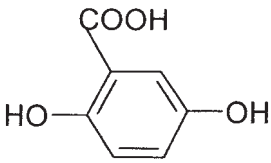 2,5-dihydroxybenzoic acid	microsomes of rat and guinea pig	47
7	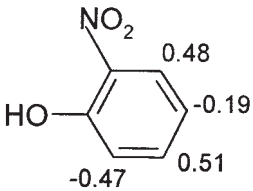 *ortho*-nitrophenol	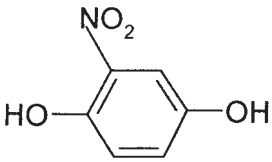 nitroquinone	rabbit	53

(*continued*)

influence of the steric effects due to the bulky substituent present in this molecule. The ΔE value for formation of the *meta*-phenol is 4 kcal/mol higher, and this metabolite is not observed experimentally.

There are four possible hydroxylation positions in the molecule 10 with OH- and HOOC-substituents; however, the calculations show that the enzyme induced hydroxylation should take place in the *ortho*- and *para*-positions relative to the OH-group, which is known to be the strongest ortho/para-directing substituent in the electrophilic substitution reactions. The ΔE_{ortho} energy is one of the lowest in the dataset, and corresponding metabolites were observes in the numerous in vivo and in vitro experiments using different test objects. In this compound, the unstable intermediate corresponds

TABLE VI
(Continued)

No	Phenols and values of ΔE	Product of hydroxylation	Condition of experiment	Reference
8	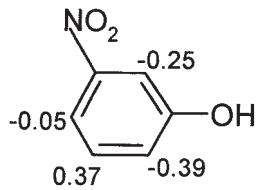 *meta*-nitrophenol	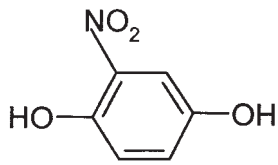 nitroquinone 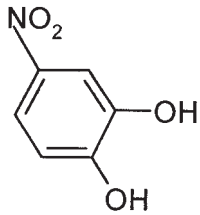 4-nitrocatechol	rabbit	53
9	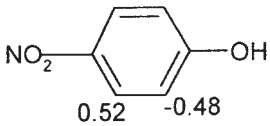 *para*-nitrophenol	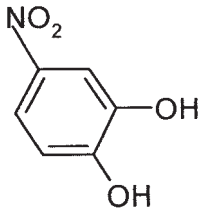 4-nitrocatechol	rabbit	53
10	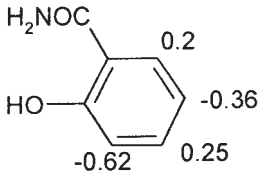 *ortho*-hydroxybenzamide	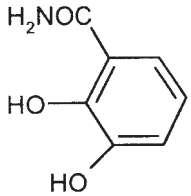 2,3-dihydroxybenzamide 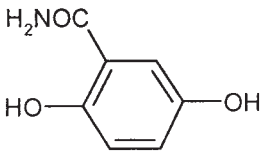 2,5-dihydroxybenzamide	rabbit	53

(*continued*)

to the *ortho*-position to the HOOC-group, which is the strong *ortho*- and *para*-deactivating (*meta*-directing) substituent, and this metabolite is not observed. In one experiment, the metabolite with OH-group in the *meta*-position to the OH-group and in the *para*-position relative the HOOC-group was observed. Formation of this metabolite is hindered in comparison to that of benzene (ΔE is positive). Unfortunately, there are no experimental quantitative estimates of feasibility of this metabolism reaction and, possibly, there are only the traces of this metabolite.

For all possible positions of hydroxylation of the compounds 11 and 12, the ΔE values only slightly differ from that of our reference compound benzene. All possible aromatic hydroxylation products are observed in vivo and in vitro experiments.

TABLE VI
(Continued)

No	Phenols and values of ΔE	Product of hydroxylation	Condition of experiment	Reference
11	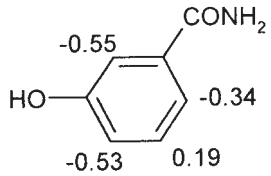 *meta*-hydroxybenzamide	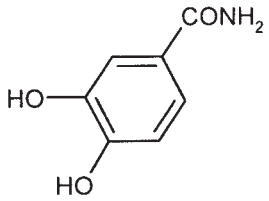 3,4-dihydroxybenzamide	rabbit	53
		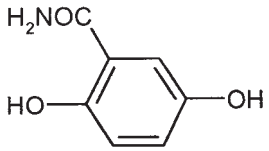 2,5-dihydroxybenzamide	rabbit	53
		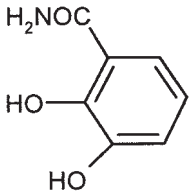 2,3-dihydroxybenzamide	rabbit	53
12	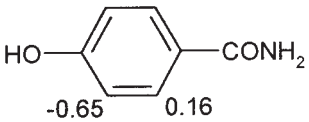 *para*-hydroxybenzamide	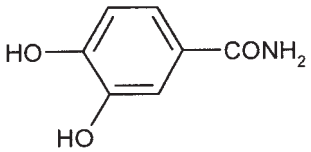 3,4-dihydroxybenzamide	rabbit	53
13	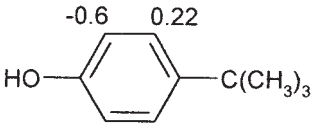 *para*-tret-butylphenol	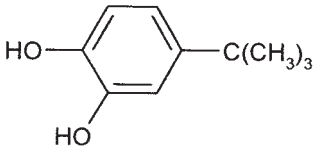 *para*-tret-butylcatechol	unspecified	46, 53
14	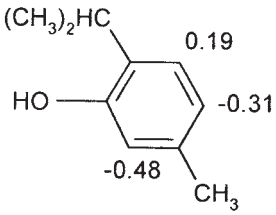 3-methyl-6-isopropylphenol	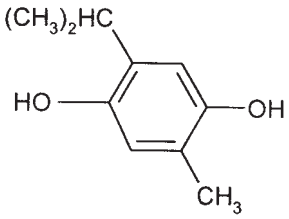 3-methyl-6-isopropyl-4-hydroxyphenol	unspecified	53

(*continued*)

There are two activating substituents in the compound 13. The hydroxylation takes place in the *ortho*-position to the stronger activating OH-group.

The hydroxylation position in the *para*-positions of the benzene rings is energetically more favorable and is observed experimentally for the compound 14.

TABLE VI
(Continued)

No	Phenols and values of ΔE	Product of hydroxylation	Condition of experiment	Reference
15	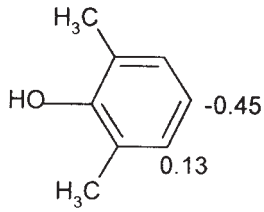 2,6-dimethylphenol	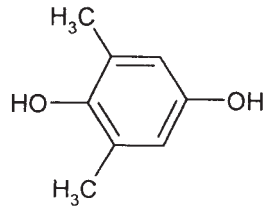 2,6-dimethylhydroquinone	unspecified	53
16	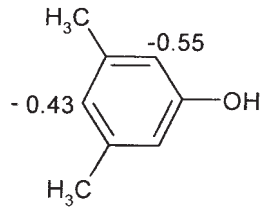 3,5-dimethylphenol	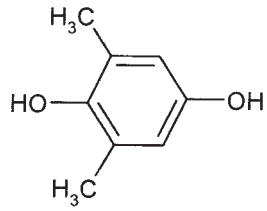 3,5-dimethylhydroquinone	unspecified	53

According to the calculations of the compound 15, the hydroxylation in the *meta*-position is favorable, and this metabolite is observed in the experiments. However, the ΔE_{para} and ΔE_{ortho} energies are only slightly larger than the ΔE_{meta}, and the corresponding *para*- and *ortho*-phenols are also detected.

For the compound 16, the hydroxylation in the *para*-position is the most feasible. This is exactly the metabolite, which is observed in vivo. According to the calculations, the two other isomers should be formed too, because the differences $\Delta E_{para} - \Delta E_{ortho}$ and $\Delta E_{para} - \Delta E_{meta}$ are equal to 1 and 2 kcal/mol only. Moreover, there seem to be no significant steric obstacles for hydroxylation in the *meta*- and *ortho*-positions.

Calculations for compound 17 show that all possible positions for aromatic hydroxylation are deactivated with respect to benzene. The *ortho*-position is characterized by the strongest deactivation, and the corresponding *ortho*-phenol is not formed in the course of the metabolic process.

In the compound 18, the minimum ΔE value corresponds to hydroxylation in the *para*-position and this metabolite is observed experimentally.

There are two benzene rings in the compound 19. The RO-group is very a strong *ortho*- and *para*-activating substituent, but the carbonyl group is a deactivating substituent. In agreement with the minimum ΔE value for the compound 19, the hydroxylation takes place in the *para*-position relative to the RO-group. The corresponding metabolite is detected in different in vivo and in vitro tests. The formation of metabolite with OH-group in the *para*-position relative to the carbonyl group is energetically unfavorable, but this metabolite was detected in one experiment. As to the possible hydroxylation positions of the second benzene ring of this molecule, the minimum ΔE value corresponds to the para-position relative to the substituent and this metabolite is observed experimentally.

The *meta*-position relative to the H_3CO-group is the strongly deactivated one in the compound 20, and the metabolite with OH-group in this position is the only one not detected in several in vitro experiments.

The two ΔE values for the two possible hydroxylation positions of the compound 21 are close to each other and only slightly differ from that of benzene. It is not surprising that both metabolites of this molecule are observed in the experiments.

The chlorine atom is a deactivating substituent, and all the ΔE values for the compound 22 are higher than the $\Delta E = 0$ value of benzene; the metabolite of the compound 22 corresponding to the highest ΔE value is not observed experimentally.

In vitro experiments detect only the *para*-product of the aromatic hydroxylation of the compound 23. According to the calculation, the lowest ΔE value corresponds to the *meta*-hydroxylation, but the difference $\Delta E_{para} - \Delta E_{meta}$ is equal only 2.4 kcal/mol.

TABLE VII

Structure of substrates of aromatic hydroxylation, the ΔE values for possible positions of hydroxylation, and experimental data (plus and minus signs correspond to the detected and undetected metabolites) together with conditions of in vivo and in vitro experiments.

No	Compound	Possible sites of hydroxy-lation	Δ*E* (kcal/mol)	Experiment	Species and route of administration or isoform of the cytochrome P450 for the direct enzyme induced oxidation
1	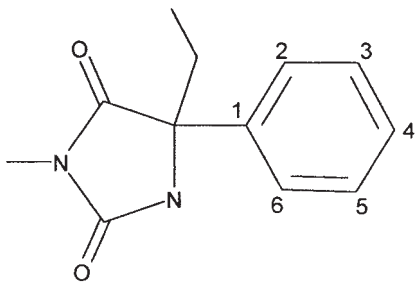	4	3.49	+	1) human, in vivo, oral, CYP2C19; 2) in vitro (human liver microsomes), CYP2C19; 3) in vitro (rat, mouse, rabbit, dog, monkey liver microsomes)
		2	12.83	−	
		3	3.71	−	
2	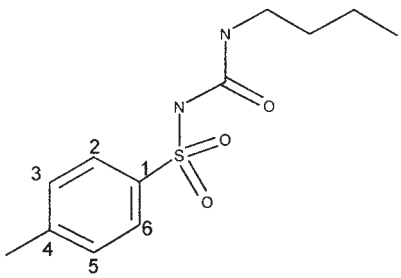	5	5.33	+	in vitro (human liver microsomes), CYP2C8, CYP2C9
		6	11.83	−	
3	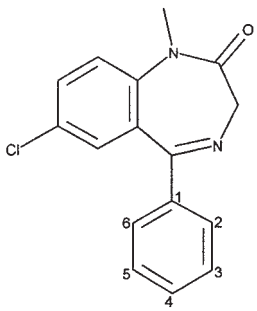	4	2.15	+	1) human (intravenous) 2) in vitro (human liver cytosol); 3) in vitro (human liver microsomes, CYP3A); 4) rat (oral, intravenous); 5) in vitro (rat liver microsomes); 6) in vitro (guinea pig hepatocytes); 7) in vitro (rabbit hepatocytes).
		5	7.65	−	
		6	2.65	−	
4	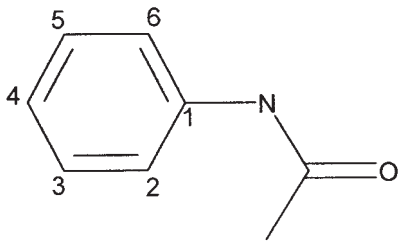	4	−4.84	+	1) human (oral); 2) in vitro (human liver microsomes); 3) β-lymphoblastoid cells expressing human CYP1A2); 4) in vitro (mouse, rat, dog liver microsomes, CYP1A2); 5) rabbit.
		3	5.71	−	
		2	−4.38	+	in vitro (mouse liver microsomes)

(*continued*)

TABLE VII
(Continued)

No	Compound	Possible sites of hydroxy-lation	ΔE (kcal/mol)	Experiment	Species and route of administration or isoform of the cytochrome P450 for the direct enzyme induced oxidation
5	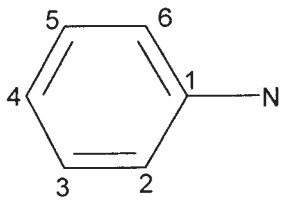	4	−15.67	+	1) in vitro (human liver microsomes), CYP2E1. 2) rat oral, intraperitoneal; 3) in vitro (rat, mouse, rabbit, dog liver microsomes), CYP2E1, CYP1A2; 4) in vitro (dog liver microsomes, CYP1A1, CYP1A2, CYP2B1, CYP2E1; 5) in vitro (rat microsomes, CYP2C11, CYP2E1)
		2	−19.83	+	1) human, rat, rabbit (oral); 2) in vitro (rainbow trout hepatocytes).
		3	−1.33	+	in vitro (human liver microsomes, CYP2E1, CYP2E2)
6	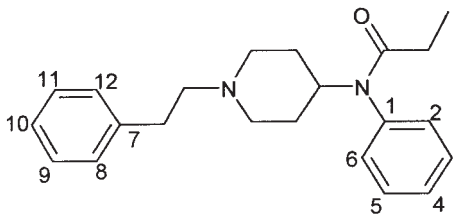	10	0.57	+	1) rat (intravenous); 2) in vitro (human, rat liver microsomes, CYP1A); 3) guinea pig liver hepatocytes
		12	7.7	−	
		11	2.3	−	
		4	−0.5	+	rat (intravenous)
		5	8.97	−	
		6	5.97	−	
7	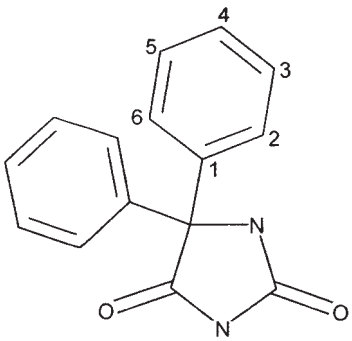	2	0.55	+	in vitro (human, rat, dog liver microsomes);
		3	1.81	+	1) horses intravenous; 2) in vitro (human placenta microsomes); 3) in vitro (dog liver microsomes CYP2C9); 4) in vitro (mouse liver microsomes)
		4	2.59	+	1) human (oral); 2) in vitro (human liver microsomes; CYP2C9, CP2C19); 3) in vitro (Hep G2 cells expressing human isoenzymes CYP2C8, CYP2C9); 4) horse oral; 5) horse intravenous;

(*continued*)

TABLE VII (Continued)

No	Compound	Possible sites of hydroxy-lation	ΔE (kcal/mol)	Experiment	Species and route of administration or isoform of the cytochrome P450 for the direct enzyme induced oxidation
8	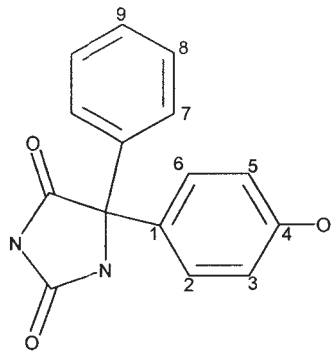	5	−0,44	+	1) in vivo human, monkey, dog; 2) in vivo mouse (intraperitoneal); 3) in vitro (human liver microsomes, CYP2C19, CYP2C9, CYP3A4, CYP3A5, CYP3A7);
		2	8.31	−	
9	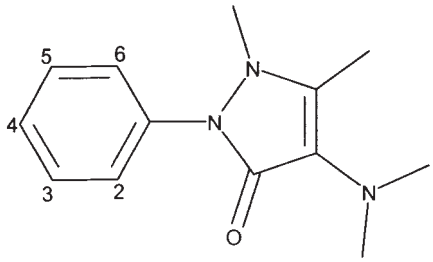	4	0.32	+	in vitro (rat, chicken liver microsomes)
		5	4.53	−	
		6	1.32	−	
10	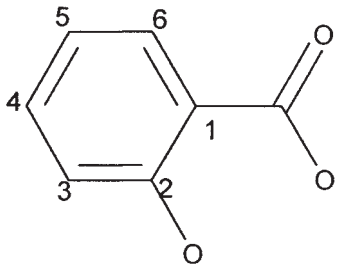	5	−2.68	+	1) human, rat, dog, rabbit (oral); 2) in vitro (human β-lymphoblastoid cells expressing human C YP3A4); 3) in vitro (human liver microsomes, CYP3A4, CYP2E1)
		6	18.77	−	
		4	5.81	+	human (oral)
		3	−9.95	+	1) rat, mouse (intra-peritoneal); 2) in vitro (human platelet homogenate); 3) in vitro (human liver microsomes)
11	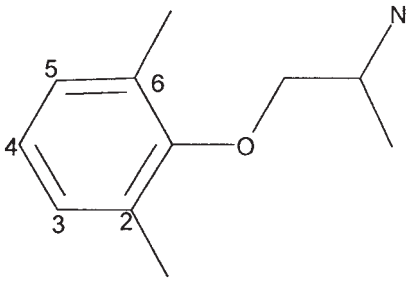	4	−3.27	+	1) human (oral, CYP2D6); 2) human (intravenous); 3) in vitro (human liver microsomes, CYP1A2, CYP2D); 4) in vitro (human β-lymphoblastoid cell microsomes expressing human CYP isoenzymes CYP2D6, CYP1A2)
		5	0.51	+	1) human (oral, CYP2D6); 2) in vitro (rat, mouse, rabbit, hamster, guinea pig liver microsomes)

(*continued*)

TABLE VII
(Continued)

No	Compound	Possible sites of hydroxy-lation	ΔE (kcal/mol)	Experiment	Species and route of administration or isoform of the cytochrome P450 for the direct enzyme induced oxidation
12	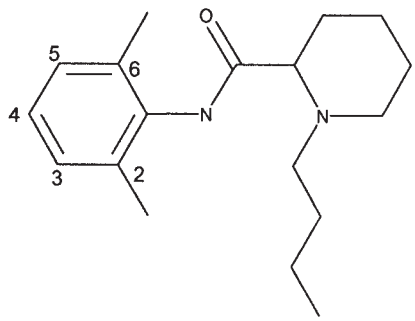	3	0.34	+	1) human (intravenous); 2) in vitro (human liver microsomes, CYP1A2);
		4	0.84	+	1) in vitro (human liver microsomes, CYP1A2); 2) human (intravenous); 3) rabbit, monkey (subcutaneous)
13	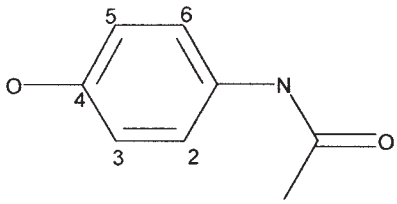	3	−11.02	+	human (oral)
		2	−4.47	−	
14	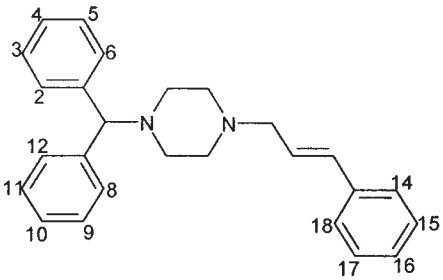	16	−0.83	+	rat (oral)
		4	0.27	+	in vitro (rat liver microsomes, CYP2D6)
		18	0.57	−	
		17	0.37	−	
		8	7.17	−	
		9	1.17	−	
15	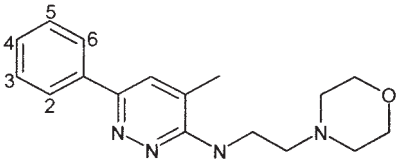	4	1.94	+	1) human, monkey, rat (oral); 2) in vitro (mouse liver microsomes, CYP2D); 3) in vitro (rat, dog, monkey liver microsomes)
		6	3.63	+	human, rat, dog (oral)
		5	−0.16	+	rat, oral
16	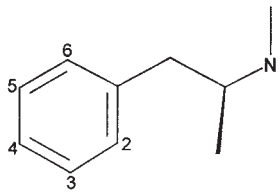	4	−0.42	+	1) human, rat (oral) 2) mouse, rat (intraperitoneal)
		2	0.83	−	
		3	1.82	−	

(*continued*)

TABLE VII (Continued)

No	Compound	Possible sites of hydroxy-lation	ΔE (kcal/mol)	Experiment	Species and route of administration or isoform of the cytochrome P450 for the direct enzyme induced oxidation
17	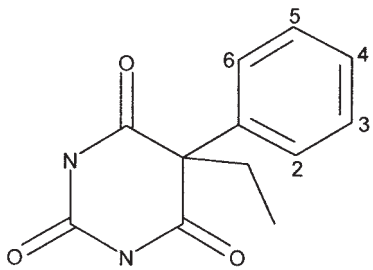	4	4.64	+	1) human, rat (oral); 2) human, rat, (intravenous); 3) in vitro (human liver microsomes, CYP2C9, CYP2C19, CYP2E1)
		6	6.3	−	
		5	4.14	+	rat (intravenous)
18	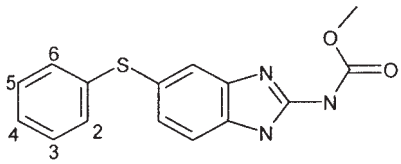	4	0.82	+	in vitro (rat liver microsomes, CYP2C11, CYP2C6, CYP2B1)
		6	7.38	−	
		5	2.55	−	
19	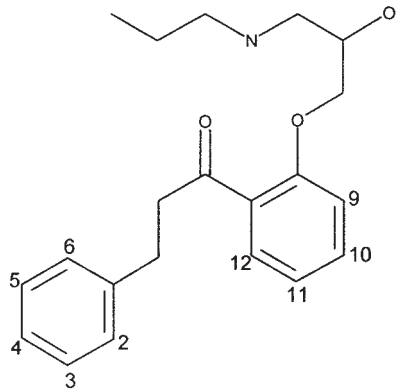	11	−2.69	+	human (oral, CYP2D6)
		12	14.91	−	
		10	7.91	+	human (oral)
		9	2.51	−	
		2	4.13	−	
		3	8.83	−	
		4	3.81	+	1) dog (oral); 2) in vitro (rat liver hepatocytes)
20	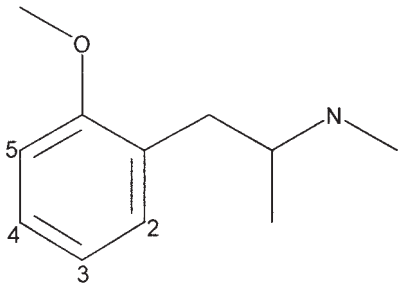	4	0.90	+	in vitro (human cytochrome P450, CYP2D6)
		5	−2.43	+	in vitro (human β-lymphoblastoid cells, CYP2D6)
		3	−2.45	+	in vitro (human β-lymphoblastoid cells, CYP2D6)
		2	7.14	−	
21	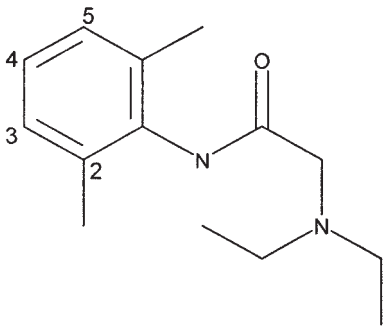	3	1.07	+	1) human, rat (oral); 2) rat, dog (intravenous); 3) in vitro (human liver microsomes, CYP1A2, CYP4A4); 4) in vitro (human β-lymphoblastoid cells, CYP2D6); 5) in vitro (rat liver and kidney microsomes, CYP2D); 6) in vitro (rat liver, kidney, lung, brain microsomes, CYP3A)
		4	−0.33	+	human, rat

(*continued*)

TABLE VII
(Continued)

No	Compound	Possible sites of hydroxy-lation	ΔE (kcal/mol)	Experiment	Species and route of administration or isoform of the cytochrome P450 for the direct enzyme induced oxidation
22	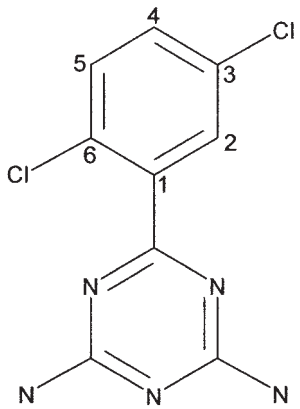	4	3.70	+	1) in vitro (human, rat, dog, monkey liver microsomes); 2) in vitro (human lymphoblast cell, microsomes expressing human CYP1A1, CYP3A4, CYP2B6, CYP1A2, CYP2C9, CYP2E1, CYP2D6)
		2	12.90	−	
		5	3.05	+	rat, dog (oral, intravenous)
23	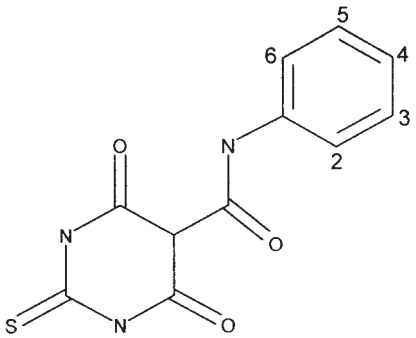	4	3.65	+	in vitro (rat liver microsomes)
		6	4.93	−	
		5	1.25	−	
24	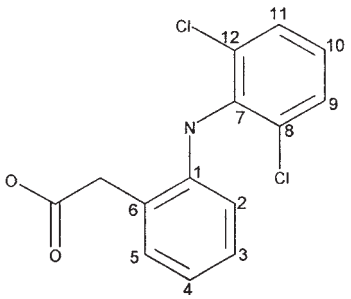	4	−0.56	+	1) human (oral); 2) in vitro (human liver microsomes, CYP3A4); 3) in vitro (human hepatocytes)
		5	5.14	−	
		3	1.15	+	in vitro (human liver microsomes, CYP2C9)
		2	−0.45	−	
		10	−1.81	+	1) human (oral); 2) in vitro (human, rat hepatocytes); 3) in vitro (HYP G2 cells, expressing human CYP2C9-Cys144); 4) in vitro (HYP G2 cells, expressing human P450 isoenzymes CYP2C9-Arg144, CYP2C9-Leu359)
		11	2.51	+	1) human (oral, intramuscular, intravenous); 2) in vitro (human hepatocytes, CYP2C9)

TABLE VIII

Experimental data [50, 51] on degradation of eight PCB congeners by eight bacterial strains: amount of primary degradation in percent after 24 h incubation, the attacked ring (right or left; r > l: both rings are attacked, the right ring being oxidized easier than the left one; r,l: both rings are oxidized with approximately equal intensity), and the theoretical minimal values of activation energy *E*(min) for the oxygen addition to the carbon atoms of benzene rings.

PCB congener	Strains								ΔE_{min} (kcal/mol)
	H1130	H430	Pi434	H201	MB1	H336	H850	LB400	
2,3-Dichloro-biphenyl	80–100 right	80–100 right	80–100 right	80–100 right	60–79 right	80–100 right	80–100 right	80–100 right	−0.41
2,3′-Dichloro-biphenyl	60–79 right	60–79 right	40–59 r > l	60–79 r > l	60–79 right	80–100 l > r	80–100 l > r	80–100 l > r	0.2
2,3′,3′-Trichloro-biphenyl	60–79 right	20–39 right	40–59 right	40–59 right	40–59 right	20–39 right	40–59 right	60–79 Right	2.5
2,5,3′-Trichloro-biphenyl	<20 right	<20 right	<20 right	<20 right	<20 right	<20 right	80–100 l > r	60–79 l > r	2.4
2,4′-Dichloro-biphenyl	20–39 right	20–39 right	40–59 r > l	40–59 r > l	<20 right	60–79 r, l	80–100 left	80–100 left	0.1
2,4,4′-Trichloro-biphenyl	60–79 right	60–79 right	40–59 right	80–100 right	40–59 right	60–79 r > l	20–39 left	40–59 l > r	1.4
3,4,2′-Trichloro-biphenyl	40–59 left	20–39 left	40–59 left	20–39 left	20–39 left	<20 right	40–59 right	60–79 right	1.2
3,3′-Dichloro-biphenyl	0	0	0	<20	40–59	0	<20	<20	1.6

For the compound 24 containing two benzene rings, the minimum ΔE values correspond to the *para*-hydroxylation to the bridging NH-group, and these products are detected experimentally.

Biodegradation of Polychlorinated Biphenyls

The contamination of the environment by polychlorinated biphenyls (PCBs) concerns virtually all the biosphere. The persistence of PCBs in the environment generates a need for a search of bacteria able to effectively degrade these compounds. The PCBs degradation by aerobic bacteria have been studied intensively [50, 51], and many bacterial strains able to degrade PCBs were found. The degradation of PCBs by bacteria results from a complex multistage process [50–52]. On the first step, the PCBs are oxidized to diols by an oxygenase enzyme system of bacteria. An intimate mechanism of the diol formation is yet not clear; however, the mechanism including a successive introduction of the oxygen atoms into the C-H bonds is under consideration [50, 51]. We proceed from the assumption that an efficiency of biodegradation process is determined by the rate of introducing of the first O atom into the substrates.

The metabolism of eight di- and trichlorobiphenyls by eight bacterial strains was studied experimentally [50, 51]. The data reflecting the facility of primary degradation of the PCBs congeners are presented in Table VIII. As may be seen from the Table, the features of the PCBs degradation depend both on the nature of the strain and the structure of the chlorinated hydrocarbon. The experimental data indicate that the five strains H1130, H430, Pi434, H201, and MB1 are able to attack the 2,3-positions of biphenyl rings only. The strains H850, LB400, and possibly H336 attack the 3,4-positions. Our aim is to describe the dependences of the facility of PCBs biodegradation on the activation energies (ΔE) of the reaction of oxygen addition to various positions of the biphenyl core (Fig. 4).

For the 2,3-dichlorobiphenyl, all positions of the unsubstituted right ring are strongly activated relative to the substituted left one, and all strains attack the right ring. This compound must be hydroxylated most easily in the series of PCBs congeners mentioned in excellent agreement with the experimental data (Table VII). For the 2,3′-dichlorobiphenyl, ΔE_{min} = 0.2 kcal/mol and corresponds

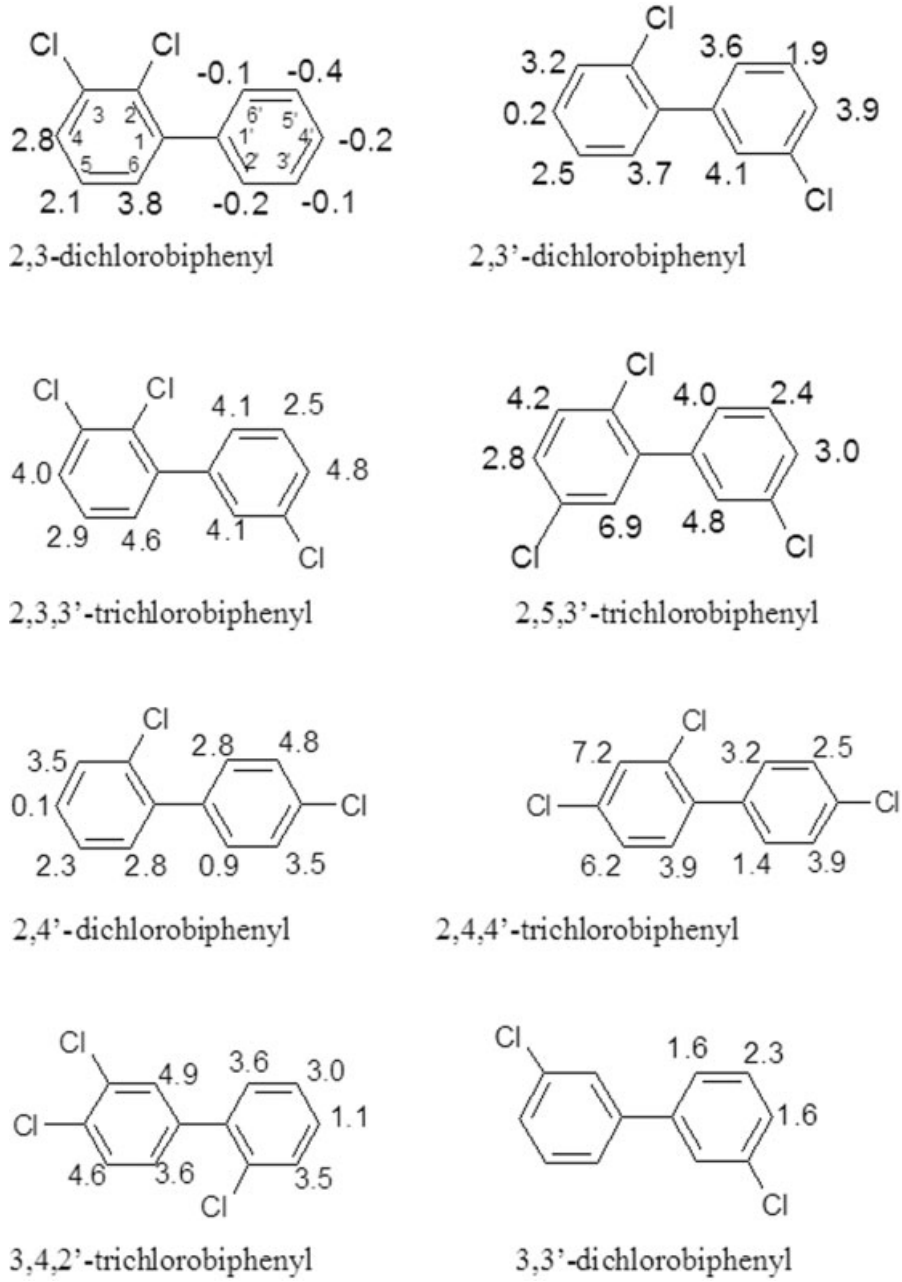

FIGURE 4. Formation energies of tetrahedral intermediates.

to the position 4 of the left ring. This is the reason why this congener is easier degraded by the H850, LB400, and H336 strains able to attack the *para*-position of the biphenyl core. The remaining five strains attack mainly the right ring containing a carbon atom with the second in magnitude barrier for the oxygen addition (ΔE = 1.9 kcal/mol). The degradation is less effective in this case. For the 2,3,3′-trichlorobiphenyl ΔE_{min} = 2.5 kcal/mol corresponds to the position 3 of the right ring and all the strains introduce the oxygen atom just into this position. For the 2,5,3′-trichlorobiphenyl, the position 3 of the right ring is the most activated one with ΔE_{min} = 2.4 kcal/mol, and all strains oxidize the right ring. The next ΔE value equal to 2.8 kcal/mol corresponds to the position 4 of the right ring. Therefore, the strains H850 and LB400 oxidize the left ring in addition to the right one. For the 2,4-

dichlorobiphenyl, very low value of ΔE_{min} equal to 0.1 kcal/mol corresponds to the position 4 of the left ring, and the strains H850 and LB400 able to attack the position 4 oxidize this PCB congener very actively, just the left ring being oxidized. The next in magnitude value $\Delta E = 0.9$ kcal/mol corresponds to the *ortho*-position of the right ring, and the strains from H1130 to MB1 oxidize the right ring. The degradation of this congener by the strain H336 reflects the features of degradation by the strains of two types. For the 2,4,4′-trichlorobiphenyl $\Delta E_{min} = 1.4$ kcal/mol corresponds to the position 2 of the right ring. Therefore, the five strains of the first type able to attack the 2,3-positions only are more active in the degradation of this congener, and the right ring is metabolized in experiment. In the case of 3,4,2′-trichlorobiphenyl, the $\Delta E_{min} = 1.1$ kcal/mol and corresponds to the position 4 of the right ring, and the strains H850 and LB400 attack the right ring. The molecule of 3,3′-dichlorobiphenyl is symmetric; the $\Delta E_{min} = 1.6$ kcal/mol corresponds both to *ortho*- and *para*- positions of the rings. Therefore, the congener must be degraded with equal facility by the strains of all types. The ΔE_{min} value is rather high, and the degradation is slow. Thus, the features of metabolism of eight di- and trichlorinated biphenyls by bacteria are described on the basis of quantum chemical calculations of the activation energies of the reaction of oxygen atom addition to various positions of biphenyl core.

References

1. Goldstein, J. A.; Faletto, M. B. Environ Health Persp 1993, 100, 169.
2. Guengerich, F. P. Chem Res Toxicol 2001, 14, 612.
3. Guengerich, F. P.; Shimada, T. Chem ResToxicol 1991, 4, 391.
4. Miller, E. C.; Miller, J. A. Pharmacol Rev 1966, 18, 805.
5. Miller, E. C.; Miller, J. A. Cancer 1981, 47, 2327.
6. McKinney, J. D. Environ Health Persp 1996, 104, 810.
7. Lag, M.; Omichinski, J. G.; Dybing, E. Chem-Biol Interact 1994, 93, 73.
8. Loew, G. H.; Spangler, D.; Spanggord, R. J. In QSAR in Toxicology and Xenobiochemistry; Tichy, M., Ed.; Pharmacochem Library; Elsevier: Amsterdam, 1985, 8, 111.
9. Ford, G. P. J Mol Struct (Theochem) 1997, 401, 253.
10. Grogan, J.; De Vito, S. C.; Korzekwa, K. R. Chem Res Toxicol 1992, 5, 548.
11. Von Szenpaly, S. V. J. J Am Chem Soc 1984, 106, 6021.
12. Lehner, A. F.; Horn, J.; Flesher, J. W. J Mol Struct (Theochem) 1996, 366, 203.
13. Flesher, J. W.; Horn, J.; Lehner, A. F. J Mol Struct (Theochem) 1996, 362, 29.
14. Noor Mohammad, S. Indian J Biochem Biophys 1984, 21, 269.
15. Braga, R. S.; Barone, P. M.; Galvao, D. S. J Mol Struct (Theochem) 1999, 464, 257.
16. Rabinowitz, J.; Little, S.; Brown, K. Int J Quant Chem 2002, 88, 99.
17. Silverman, B. D. Cancer Biochem Biophys 1981, 5, 207.
18. Maynard, A. T.; Pedersen, L. G.; Posner, H. S.; McKinney, J. D. Mol Pharmacol 1986, 9, 629.
19. Loew, G. H. Sudhidra, B. S.; Burt, S. Int J Quant Chem: Quant Biol Symp 1979, 6, 259.
20. Sabbioni, G.; Wild, D. Carcinogenesis 1992, 13, 709.
21. Wild, D. Environ Health Persp 1993, 88, 27.
22. Ford, G. P.; Herman, P. S. Chem-Biol Interact 1992, 9, 81.
23. Hatch, F. T.; Colvin, M. E.; Seidl, E. T. Environ Mol Mutagen 1996, 27, 314.
24. Benigni, R.; Passerini, L. Mutat Res 2002, 511, 191.
25. Benigni, R.; Andreoli, C. Environ Mol Mutag 1994, 24, 208.
26. Sasaki, J. C.; Fellers, R. S.; Colvin, M. E. Mutat Res 2002, 506, 79.
27. Pudzanowski, A. T.; Loew, G. H.; Mico, B. A. J Am Chem Soc 1983, 105, 3434.
28. Quanhuan, D. J Mol Struct (Theochem) 1987, 149, 167.
29. Loew, G. H.; Rebagliati, M.; Poulsen, M. Biochem Biophys 1984, 7, 109.
30. Korzekwa, K. R.; Jones, J. P.; Gilette, J. R. J Am Chem Soc 1990, 112, 7046.
31. Yin, H.; Anders, M.; Korsekwa, K.; Higgins, L. A.; Thummel, K. E. Proc Natl Acad Sci USA 1995, 92, 11076.
32. Parke, D. V. The Biochemistry of Foreign Compounds; Pergamon Press: Oxford, 1968; p 120.
33. Rickert, D. E. Drug Metabol Rev 1987, 18, 23.
34. Hata, M.; Hoshino, T.; Tsuda, M. Chem Commun 2000, 2037.
35. Hata, M.; Hirano, Y.; Hoshino, T.; Nishida, R.; Tsuda, M. J Mol Struct (Theochem) 2005, 722, 133.
36. de Visser, S. P.; Ogliaro, F.; Sharma, P. K.; Shaik, S. J Am Chem Soc 2002, 124, 11809.
37. de Visser, S. P.; Shaik, S. J Am Chem Soc 2003, 125, 7413.
38. Bathelt, C. M.; Ridder, L.; Mulholland, A. J.; Harvey, J. N. J Am Chem Soc 2003, 125, 15004.
39. Bathelt, C. M.; Ridder, L.; Mulholland, A. J.; Harvey, J. N. Org Biomol Chem 2004, 2, 2998.
40. Dowers, T. S.; Rock, D. A.; Rock, D. A.; Perkins, B. N.; Jones, J. P. Drug Metabol Dispos 2004, 32, 328.
41. Yuan, Z. X.; Kumar, S.; Sikka, H. C. Chem Res Toxicol 2004, 17, 672.
42. Korsekwa, K.; Trager, W.; Gouterman, M.; Spangler, D.; Loew, G. H. J Am Chem Soc 1985, 107, 4273.
43. Burka, L. T.; Plucinski, T. M.; McDonald, T. L. Proc Natl Acad Sci USA 1983, 80, 6680.
44. Pudzianowski, A. T.; Loew, G. H. J Mol Catal 1982, 17, 1.
45. Pudzianowski, A. T.; Loew, G. H. Int J Quantum Chem 1983, 23, 1257.
46. Kuznetsov, A. V. Molekulyarnaya Biologiya (Molecular Biology) 1990, 24, 1373 [in Russian].
47. Daly, J.; Jerina, D.; Witkop, B. Arch Biochem Biophys 1968, 128, 517.

48. Novikov, S. M.; Poroikov, V. V.; Tertychnikov, S. N. Gygiena i Sanitariya (Hygiene and Sanitary) 1995, 1, 29 [in Russian].
49. Hanch, C.; Leo, A. J. Substituents Constants for Correlation Analysis in Chemistry and Biology. Wiley: New York, 1979.
50. Bedarl, D. L.; Haberl, M. L. Microbiol Ecol 1990, 20, 87.
51. Bedarl, D. L.; Haberl, M. L. Appl Environ Microbiol 1987, 53, 1103.
52. Chakrabarty, A. M. Biodegradation and Detoxication of Environmental Pollutants, CRC Press: Boca Raton, FL, 1982; p 39.
53. Williams, R. T. Detoxication Mechanisms. The Metabolism and Detoxication of Drugs, Toxic Substances and Other Organic Compounds. Chapman & Hall: London, 1959.
54. Rusvai, E.; Vedh, M.; Kramer, M. Biochem Pharmacol 1988, 37, 4574.
55. Loew, G. H.; Sudhindra, B. S.; Walker, J. M. J Environ Pathol Toxicol 1979, 2, 106.
56. Inoue, O.; Seiji, K.; Ikeda, M. Bull Environ Contam Toxicol 1989, 43, 220.
57. Gorrod, J. W. Xenobiotica 1980, 10, 603.
58. Nechiporenko, S. P.; Rotenberg, Yu. S. Toksikologiya (Toxicology) 1981, 12, 118 [in Russian].
59. Bakke, O. M.; Scheline, R. R. Toxicol Appl Pharmacol 1970, 691.
60. Woiwode, W.; Wadarz, R.; Drysch, K.; Weichardt, H. Arch Toxicol 1979, 43, 93.
61. Woiwode, W.; Drysch, K. Br J Ind Med 1981, 38, 194.
62. Kondo, K. Yoshido, Y.; Yamadata, H. Ind Health 1985, 23, 37.
63. Hanzlik, R. P.; Hogberg, K.; Judson, C. M. Biochemistry 1984, 23, 3048.
64. Inoue, O.; Seigi, K.; Nakotsuka, H. Bull Environ Contam Toxocol 1989, 43, 74.
65. Ohtsuji, H.; Ikeda, M. Toxicol Appl Pharmacol 1971, 16, 321.
66. Ogata, M.; Shimada, Y. Int Arch Occup Environ Health 1983, 53, 51.
67. Selander, H. G.; Jerina, D. M.; Daly, J. W. Arch Biochem Biophys 1975, 168, 309.
68. Rickert, D. E. Drug Metabol Rev 1987, 18, 23.
69. Pathiratne, A.; Puyear, R. L.; Brammer, J. D. Drug Metal Dispos 1984, 14, 386.
70. Yoshida, M.; Hara, I. Ind Health 1985, 23, 239.